https://doi.org/10.5194/os-2021-7
Preprint. Discussion started: 15 February 2021

Ocean Science
Discussions
Open Access

Observational Study on the Variability of Mixed Layer Depth in the Bering Sea and the Chukchi Sea in the Summer of 2019

Xiaohui Jiao[1], Jicai Zhang[1,*], Chunyan Li[2]

[1] Institute of Physical Oceanography, Ocean College, Zhejiang University, Zhoushan 316021, China.

[2] Department of Oceanography and Coastal Sciences, College of the Coast and Environment, Louisiana State University, Baton Rouge 70803, U.S.A.

Corresponding author: Jicai Zhang (jicai_zhang@163.com)

Key Points:

- The mixed layer depth in the Bering Sea Slope was greater than that in the Bering Sea Basin due to the circulation and eddy in the slope
- The mixed layer depth was influenced by the Bering Sea Anadyr Water and the Alaska Coastal Water in the Bering Sea shelf
- The further northward, the more important role the salinity played in determining the mixed layer depth in the Chukchi Sea.

https://doi.org/10.5194/os-2021-7
Preprint. Discussion started: 15 February 2021

Abstract

Based on the high-resolution CTD data from 58 stations in the Bering Sea and the Chukchi Sea in the summer of 2019, the mixed layer depth (MLD) was obtained according to the density difference threshold method. It was verified that the MLD could be estimated more accurately by using a criterion of $0.125\ \mathrm{kg}/m^3$ in this region. The MLD in the Bering Sea basin was larger than that in the Bering Sea shelf, and both of them were smaller than that in the Bering Sea slope. The MLD increased northward both in the Chukchi Sea shelf and the Chukchi Sea slope. The farther northward, the greater the difference between the MLD calculated from temperature (MLDt) and the MLD calculated from density (MLDd) was, and the more important the role of salinity was in determining the MLD. The larger MLD (refer to MLDd specifically) in the Bering Sea slope might be due to the enhancement of mixing caused by the Bering Slope Current (BSC) and eddies. The horizontal advection of the Bering Sea Anadyr Water and the Alaska Coastal Water in the Bering Sea shelf led to the shallower MLD in the central transition zone. The northward increase of the MLD in the Chukchi Sea might be related to the low-salinity seawater resulting from the melting of sea ice in summer. The spatial variation of MLD was more closely related to the surface momentum flux than the sea surface buoyancy flux, and the wave had little effect.

https://doi.org/10.5194/os-2021-7
Preprint. Discussion started: 15 February 2021

1 Introduction

The dynamics in the Bering Sea and the Chukchi Sea have an important impact on global climate change (Hu et al., 2010). The mean sea level in the Pacific is higher than that of the Arctic Ocean (Coachman & Aagaard, 1966). Therefore, the average flow in the Bering Strait is northward (Overland et al., 1996), and the average annual flow is about 0.83 Sv (Roach et al., 1995). The net northward transport has a marked impact on Arctic sea ice, as it feeds a subsurface temperature maximum under the ice-pack in winter (Woodgate et al., 2010; Woodgate et al., 2012). It also influences the global hydrologic cycle (Serreze et al., 2006), and the global thermohaline circulation (Shaffer & Bendtsen, 1994; Wadley & Bigg, 2002). The seasonality of the northward heat and freshwater transport is strongly influenced by the mixed layer (Woodgate, 2018).

The exploration of the upper ocean mixed layer depth (MLD hereafter) will be very beneficial for the study of the northward heat and water transport through the Bering Strait and its climatic effects. Water mass formation and circulation (Hanawa & Talley, 2001; Stommel, 1979), sea-air exchange (Frankignoul & Hasselmann, 1977; Kraus & Turner, 1967; Rodgers et al., 2014; Stevenson & Niiler, 1983), biogeochemical processes (Fasham et al., 1990; Fauchereau et al., 2011; Sverdrup, 1953), transfer of heat between ocean and sea ice (Sirevaag, et al., 2011), and melting/freezing of sea ice (Polyakov et al., 2013) are highly sensitive to the variations of MLD. The mixed layer affects the process of biological production by importing or exporting phytoplankton and nutrients into the light-transmitting layer (Chen et al., 1994; Ohlmann et al., 1996). The accuracy of MLD also plays an important role in the reliability of climate model results (Belcher et al., 2012). Therefore, the exact information of MLD is vital for the study of physical oceanography, climate change, and relative subjects.

Many factors can affect the variations of MLD, such as surface heat and freshwater fluxes, horizontal advection, wind stress (Hu & Wang, 2010), Langmuir circulation (Li et al., 2013), sea ice (Peralta-Ferriz & Woodgate, 2015), eddy (Gaube et al., 2019), and the oceanographic structure including temperature and salinity below the mixed layer

https://doi.org/10.5194/os-2021-7
Preprint. Discussion started: 15 February 2021

(Hanawa & Toba, 1981; Tully, 1964). The strengthening or weakening of stratification caused by the air-sea kinetic energy exchange or buoyancy flux in the surface of the ocean will also change the MLD (Deardorff et al., 1969; Kato & Phillips, 1969; Kraus & Turner, 1967; Large et al., 1994; McWilliams et al., 1997; McWilliams et al., 2009; Price et al., 1986). Under the effect of wind, waves, and Langmuir circulation, the MLD become deeper, which has been proved by many researches based on theory, observations, and numerical models (Bruneau & Toumi, 2016; Li et al., 2013; Wu et al., 2015).

The variation of the mixed layer in this region is complicated due to the influence of the circulation, eddy, wind, and sea ice. The major current in the Bering Sea is a cyclonic circulation with the Bering Slope Current (BSC hereafter) along the Bering Sea slope, the Kamchatka Current in the northwest, the Alaskan Coastal Current in the northeast, and the Aleutian North Slope Current in the north of Aleutian Islands (Panteleev et al., 2012). A sketch of them is shown in Figure 1 (Danielson et al., 2014). The hydrological characteristics in the Bering Sea are influenced by the Pacific Ocean due to the water exchange between the Bering Sea and the Pacific Ocean with the major inflow through the Near Strait and outflow through Kamchatka Strait (Stabeno & Reed, 1994). Strong eddy activities have been observed along the Bering Slope due to the instability of the BSC (Mizobata et al., 2006; Okkonen, 2001). The seasonal variation of wind in this region is remarkable. In winter, the Aleutian Low moves southward, and most areas of the Bering Sea are controlled by polar cold air (Rodionov et al., 2007). Northwest wind prevails and part of the sea surface will be frozen (Zhang et al., 2010). In summer, south wind prevails, and all the sea ice is melted (Dong et al., 2019; Serreze et al., 2016). As a result, the MLD varies drastically in time and space. Since the Bering Sea is separated into the coastal shelf, middle shelf, outer shelf, and basin by fronts approximately overlying the 50m isobaths, 100 isobaths, and continental slope (Coachman and Charnell, 1979; Kachel et al., 2002; Kinder and Coachman, 1978; Schumacher et al., 1979), the vertical structure of the water column and physical process can be different, including the mixed layer. The upper layer is wind-mixed and the bottom layer is

https://doi.org/10.5194/os-2021-7
Preprint. Discussion started: 15 February 2021

Ocean Science
Discussions
Open Access

tidally-mixed in the middle shelf of the Bering Sea (Schumacher and Stabenow, 1998). The sea ice in the Arctic showed a trend of later freeze up and a trend toward earlier melt onset (Markus et al., 2009), which might change the temporal variation of the mixing layer. The MLD can be less than 20 m in summer while reaching more than 500 m in winter in subpolar latitudes (Monterey, 1997). Seasonal variability of the MLD is associated with heat flux in the Bering Sea (Kara et al., 2000).

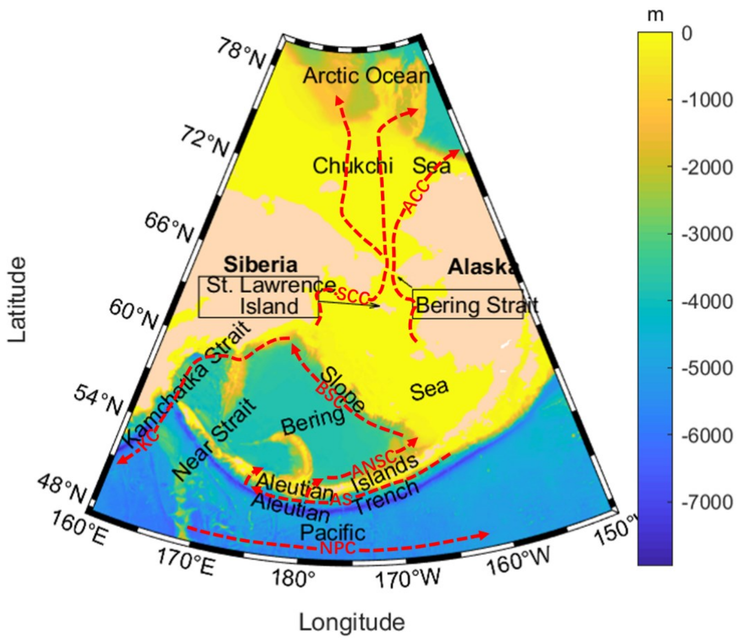

Figure 1. Topography, bathymetry, and circulation in the Bering Sea, Chukchi Sea, and adjacent region. Abbreviations include: ACC = Alaskan Coastal Current; SCC = Siberian Coastal Current; KC = Kamchatka Current; BSC = Bering Slope Current; ANSC = Aleutian North Slope Current; AS = Alaskan Stream; NPC = North Pacific Current. (Danielson et al., 2014; Kawaguchi & Nishioka, 2020)

Thanks to the rapid growth of Argo observations in the past decade, the MLD in most of the global ocean has been better studied (Holte et al., 2017). There are several global MLD datasets available (Carton et al., 2008; de Boyer Montégut et al., 2004; Hosoda et al., 2010; Monterey, 1997; Schmidtko et al., 2013). Some of them use the temperature to get the MLD without the salinity data. Besides, most of these previous works mainly focused on the global ocean, but less on the Bering Sea and the Chukchi Sea, except for the study on the MLD in the Arctic (Peralta-Ferriz & Woodgate, 2015). It was found that the overall mixed layer gradually became shallower from 1978 to 2012 by studying the seasonal and inter-annual changes of the MLD in the Arctic region (Peralta-Ferriz & Woodgate, 2015), which covered the Chukchi Sea but lacked the data in the Bering Sea. At present, due to the lack of high spatial resolution datasets and further understanding of the ocean dynamics, the global model simulation results still have large deviations (Belcher et al., 2012; D'Asaro, 2014; DuVivier et al., 2018). To evaluate and reduce the model deficiency in modeling the values of MLD, direct observations of MLD are of great significance, especially for the Arctic ocean. In this paper, the field observational data sampled during the summer of 2019 will be analyzed to study the spatial variations of MLD in the Bering Sea and the Chukchi Sea, which will benefit the model calibration and evaluation, air-sea interaction, and climate change, etc.

This paper is organized as follows. Section 2 introduces the data and methods. The analyzing results are given in Sect. 3. The processes related to the spatial variation of MLD are discussed in Sect. 4. Section 5 presents the summary and conclusions.

2 Data and methods

2.1. Study area

The Bering Strait connecting the Bering Sea and the Chukchi Sea has a depth of about 50 m and a width of 80 km and is the only direct ocean gateway for the exchange of matter and energy between the Arctic Ocean and the Pacific Ocean (Woodgate et al., 2005). The north-south span of the Bering Sea is around 1500 km and the east-west span is more than 2300 km (Figure 2). The northeast part of the Bering Sea is a shallow continental shelf, the depth of which ranges from tens of meters to about two hundred meters (Dong et al., 2019). The southwest part is a basin with a depth of more than 3000 m in most areas. A sharp change of the water depth from 200 m on the northeastern side to 2000 m on the southwestern side exists within less than 100 km in width between the Bering Sea basin and the Bering Sea shelf (Figure 2). The southern part of the Chukchi

https://doi.org/10.5194/os-2021-7
Preprint. Discussion started: 15 February 2021

Sea is a continental shelf with a depth of about 50 m (Woodgate et al., 2005), and the northern part is a basin with a depth of more than 2000 m.

2.2. Data

The in-situ observational data used in this paper were obtained during the 10th Chinese National Arctic Research Expedition from Aug. 10 to Sept. 30, 2019. As shown in Figure 2, 58 stations were distributed in BL, BR, BS, R, BT, and M transection (Figure 2). The BL section was located across the western Bering Sea basin, continental slope, and continental shelf. The BS section was located in the northern Bering Sea shelf. The BR section was located in the eastern Bering Sea slope and shelf. The R section was located in the southern Chukchi Sea shelf, and BT was located in the northern Chukchi Sea shelf. M section was located in the Chukchi Sea slope. These sections are representatives of this region.

Two kinds of observations were carried out during the expedition: transect hydrographic investigations and ship-borne ADCP observation. LADCP/CTD operations were performed to get profiles of temperature, salinity, and velocity at 58 stations (Figure 2 and Table 3) during the transect hydrographic investigations. The SBE 911 Plus (Table 1), Teledyne RDI WHMariner 300kHz, and Teledyne RDI OS 38kHz (Table 2) were used in the transect hydrographic investigations (stations in Figure 2). Ship-borne ADCP measurement was carried out while the ship was in motion to get the current profile of the upper ocean along the track. The surface temperature and salinity measurements were made as well in the underway observations. The SeaBird FerryBox (Table 1) and Teledyne RDI WHSentinel 300kHz (Table 2) were used in the underway observations.

The Lowered ADCP used to observe the current velocity was a 300 kHz Teledyne RDI WHN Workhorse Sentinel. During the observation, the descending rate of the instrument was controlled to 1.0 m/s. The signal frequency of lowered ADCP used to observe the ocean current was 300 kHz, and its max range was 110 m. The real sampling depth changes with the particles, temperature, and salinity of the seawater.

https://doi.org/10.5194/os-2021-7
Preprint. Discussion started: 15 February 2021

The vertical sampling resolution of the Lowered ADCP was 2 ~ 8 m, and the sampling frequency was 1 Hz. The Lamont-Doherty Earth Observatory (LDEO) software based on the inverse method (Visbeck, 2002) was used to process the data from the Lowered ADCP.

The temperature, conductivity, pressure, and dissolved oxygen were measured in the transect hydrographic investigations. The lowered CTD measuring the temperature and salinity was SBE-911-Plus direct-reading temperature-conductivity-depth profiler (Table 1), and the sampling frequency was 24 Hz. Since a second redundant pair of temperature, conductivity, pressure sensors, and the pump were installed, we could perform better quality control on multiple parameters.

The signal frequency of ship-based underway ADCP was 38 kHz in the basin and the continental slope and was 300 kHz in the continental shelf (Table 2). Since the depth in the continental shelf was shallow, the bottom tracking was used for better accuracy in the ocean current velocity measurements. In the deeper ocean basin and the continental slope, the velocity of the vessel calculated by GPS was used to correct the current velocity. The ship-based underway equipment for the surface temperature and salinity measurement was the SeaBird FerryBox.

184 **Table 1.** Equipment for temperature and salinity measurement.

Instrument	**Model**	**Sampling frequency**	**Conductivity resolution**	**Temperature resolution (℃)**	**Pressure resolution (db)**
Lowered CTD	SBE 911 Plus	24	0.00004	0.0002	0.001
Underway multi-element system	SeaBird FerryBox	1	0.005	0.0001	--

185

186 **Table 2.** ADCP Model

Instrument	**Model**	**Bin size**	**Sampling depth**	**No. Bins**	**Pings/Ens**	**Time/Ping(s)**
Lowered ADCP	Teledyne RDI WHSentinel 300kHz	2~8m	110m	14~50	1	1
Underway ADCP1	Teledyne RDI WHMariner 300kHz	4m	110m	50	1	0.5
Underway ADCP2	Teledyne RDI OS 38kHz	24m	960m	40	1	3

https://doi.org/10.5194/os-2021-7
Preprint. Discussion started: 15 February 2021

Table 3. The longitude, latitude, and sampling start time of the 58 stations.

Station	Longitude	Latitude	Date and time	Station	Longitude	Latitude	Date and time
BL01	171.87E	54.58N	24/08 06:33:22	**BS04**	170.13W	64.33N	29/08 08:20:48
BL02	172.77E	55.27N	24/08 13:02:20	**BS05**	169.41W	64.33N	29/08 10:11:39
BL03	174.57E	56.57N	24/08 23:36:43	**BS06**	168.71W	64.33N	29/08 12:05:17
BL04	175.60E	57.39N	25/08 07:27:26	**BS07**	168.11W	64.33N	29/08 14:01:38
BL05	177.41E	58.30N	25/08 18:03:27	**BS08**	167.45W	64.37N	29/08 15:14:42
BL06	178.41E	58.72N	27/08 00:06:14	**BT12**	167.12W	74.32N	03/09 05:54:45
BL07	179.51W	60.04N	27/08 13:46:35	**BT13**	167.82W	74.75N	01/09 08:00:24
BL08	179.00W	60.40N	27/08 17:28:25	**BT14**	167.85W	75.03N	01/09 11:17:22
BL09	178.21W	60.80N	27/08 21:38:45	**BT15**	167.82W	75.33N	01/09 14:36:37
BL10	177.23W	61.29N	28/08 02:32:42	**BT16**	167.80W	75.64N	01/09 18:11:55
BL11	176.17W	61.93N	28/08 07:25:10	**BT25**	167.81W	74.74N	02/09 20:59:52
BL12	175.01W	62.59N	28/08 12:18:21	**BT26**	171.21W	74.60N	01/09 04:20:21
BL13	173.43W	63.29N	28/08 18:19:56	**BT27**	169.32W	74.35N	03/09 09:42:37
BL14	172.40W	63.77N	28/08 22:08:49	**M11**	166.44W	74.80N	02/09 18:08:27
BR00	174.09W	56.95N	08/09 15:52:39	**M12**	172.00W	75.21N	02/09 14:48:17
BR01	173.69W	57.41N	08/09 11:26:24	**M13**	172.01W	75.61N	02/09 10:55:12
BR02	173.22W	57.90N	08/09 07:31:37	**M14**	172.00W	76.03N	02/09 02:53:16
BR03	172.73W	58.40N	08/09 04:22:07	**M15**	171.96W	75.82N	01/09 22:43:37
BR04	172.25W	58.91N	08/09 00:26:27	**R01**	169.87W	66.21N	30/08 02:09:33
BR05	171.30W	59.90N	07/09 17:25:13	**R02**	168.75W	66.89N	30/08 05:40:07
BR06	170.35W	60.91N	07/09 11:09:28	**R03**	168.75W	67.50N	30/08 09:16:57
BR07	169.67W	61.65N	07/09 06:18:06	**R04**	168.75W	68.19N	30/08 13:09:21
BR08	168.89W	62.40N	07/09 01:13:13	**R05**	168.76W	68.81N	30/08 17:17:20
BR09	168.42W	62.91N	06/09 21:16:20	**R06**	168.75W	69.53N	30/08 21:11:26
BR10	167.93W	63.40N	06/09 18:11:50	**R07**	168.75W	70.33N	31/08 02:08:10
BR11	167.47W	63.90N	06/09 14:01:53	**R08**	168.75W	71.17N	31/08 07:18:38
BS01	171.39W	64.32N	29/08 02:52:43	**R09**	168.75W	71.99N	31/08 11:56:35
BS02	170.82W	64.33N	29/08 04:42:27	**R10**	168.74W	72.90N	31/08 16:38:02
BS03	170.12W	64.33N	29/08 06:31:27	**R11**	168.74W	74.15N	31/08 23:57:32

https://doi.org/10.5194/os-2021-7
Preprint. Discussion started: 15 February 2021

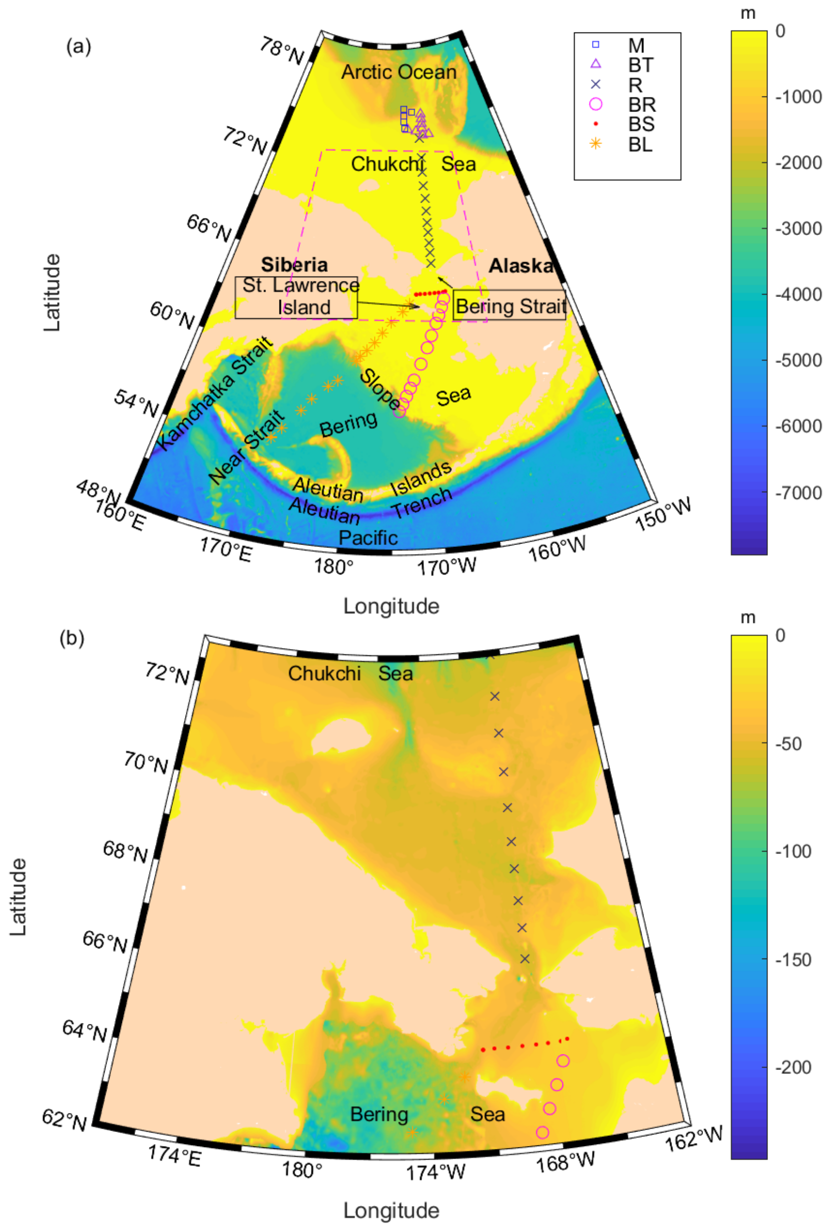

Figure 2. (a) showed the distribution of the 58 observation stations. The asterisks, dots, circles, crosses, triangle, and squares represented the BL, BS, BR, R, BT, and M transection, respectively. (b) showed the bathymetry and topography in the dashed line rectangle in (a).

https://doi.org/10.5194/os-2021-7
Preprint. Discussion started: 15 February 2021

The automatic meteorological station installed at a height of 16 m above the sea level was used to measure wind speed, air temperature, air pressure, and humidity throughout the cruise. The speed of the ship estimated by GPS was used to calculate wind speed. The sampling interval is 1 minute.

The CCMP reanalysis wind data at a height of 10 m above the sea level was also used in the present work. The spatial resolution of CCMP data is 0.25°, and the temporal resolution is 6 hours (Wentz et al, 2015). The sea surface heat flux and water flux were obtained from the CFSv2 (Saha et al., 2011). The Bering Sea level was obtained from the combined measurements of several altimeters (available online at https://resources.marine.copernicus.eu/?option=com_csw&view=details&product_id=SEALEVEL_GLO_PHY_L4_NRT_OBSERVATIONS_008_046). The significant wave height was obtained from the COPERNICUS MARINE ENVIRONMENT MONITORING SERVICE (available online at https://resources.marine.copernicus.eu/?option=com_csw&view=details&product_id=WAVE_GLO_WAV_L4_SWH_NRT_OBSERVATIONS_014_003). The bathymetric data used in this paper was from ETOPO1 (Amante & Eakins, 2009).

2.3. The criterion for the MLD

In practice, several ocean parameters, including temperature, salinity, density, turbulent mixing, and dissolved oxygen, can be used to calculate the value of MLD. Methods to estimate MLD include difference threshold (de Boyer Montégut et al., 2004), gradient threshold (Lukas & Lindstrom, 1991), curvature method (Lorbacher et al., 2006), split and merge method (Thomson & Fine, 2003), etc. For example, the potential density difference threshold method was used to calculate the MLD with a criterion of 0.01 kg m^{-3} and a reference depth of 10 m (Smyth et al., 1996; Wijesekera & Gregg, 1996). The potential density gradient threshold method determined the MLD as a depth range where the vertical gradient of the potential density was below a critical value, and many researchers used a gradient threshold of $0.1\ \ \mathrm{kg}/m^4$ (Lukas & Lindstrom, 1991). The MLD calculated by the least-squares regression and integration method represented the

https://doi.org/10.5194/os-2021-7
Preprint. Discussion started: 15 February 2021

depth of the thermocline to a greater extent. Some researchers proposed a split-and-merge method, which could be used not only to calculate the MLD but also to describe other marine vertical structural features (Thomson & Fine, 2003). Therefore, the difference threshold and gradient threshold are better choices. Although dissolved oxygen could be used to calculate MLD, the results are not accurate where Ekman pumping is strong or marine productivity is active. Besides, due to the existence of the vertical density-compensated layer, the MLD estimated by density maybe not accurate in winter (de Boyer Montégut et al., 2004).

In this paper, the most widely adopted difference threshold method was used to estimate the MLD. The criterion was critical as the small vertical fluctuations of the temperature (red rectangle in Figure 3 (b)) and density within the mixed layer might bring confusion when calculating the MLD. The temperature profiles of all stations could be divided into three classes. BR01 was a station of type A, where the temperature of the mixed layer was almost completely homogeneous, and the temperature gradient was very small. BR00 was a station of type B, where the temperature of the mixed layer had local extremum. As a result, if a small threshold was used, the calculated MLD would be shallower than the real MLD. BL08 was a station of type C, and the temperature of the mixed layer changed significantly vertically. In general, the temperature had an apparent trend of decreasing with depth, and small amplitude fluctuations were imposed on this trend.

https://doi.org/10.5194/os-2021-7
Preprint. Discussion started: 15 February 2021

Ocean Science
Discussions
Open Access

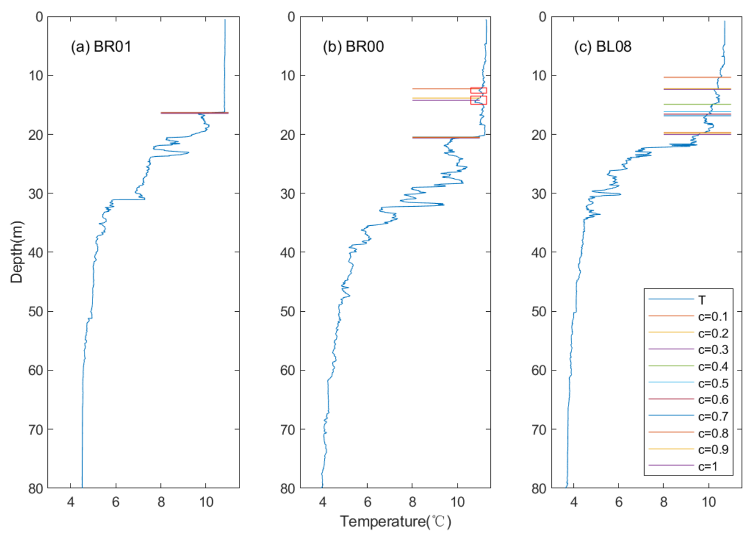

Figure 3. Three types of temperature profiles. Horizontal lines in different colors showed different MLDs responding to a group of temperature criteria. (a) showed the type A temperature profile, which had almost the same MLD using different criteria. (b) showed the type B temperature profile, and the MLD calculated from this temperature profile using different temperature criteria was distributed around the local extremum. (c) showed the type C temperature profile; the MLD calculated from type C temperature profile using different temperature criteria had more difference, and the distributions were more dispersed. The variable c in the legend represented the temperature criteria which ranged from 0.1 to 1 ℃.

As Figure 3 and Figure 4 showed, the MLD could be divided into three types as well. The type A stations had almost the same MLD using different criteria. The MLD calculated from type B stations using different temperature criteria was distributed around the local extremum. The MLD calculated from type C stations using different temperature criteria had more difference, and the distributions were more dispersed.

A criterion that could overcome the influence of the local extremum was used in the Bering Sea and the Chukchi Sea. The suitable criterion for the temperature difference method was 0.5 ℃. To explore the role of temperature and salinity in the spatial variation of the MLD, the MLDd (MLD from the density) and the MLDt (MLD from the temperature) were both calculated, and in the following, MLD specifically refers to MLDd. The density profiles at some stations also had local extremum, and the same

https://doi.org/10.5194/os-2021-7
Preprint. Discussion started: 15 February 2021

principle was followed in determining the criterion for the density difference method. The MLDd was defined as the depth at which density differed from that of the depth of 5 m by 0.125 kg/m^3. This is consistent with the previous research. Considering the diurnal variation of MLD, the criteria may be 0.125 kg/m^3 in climate research (Kara et al., 2000).

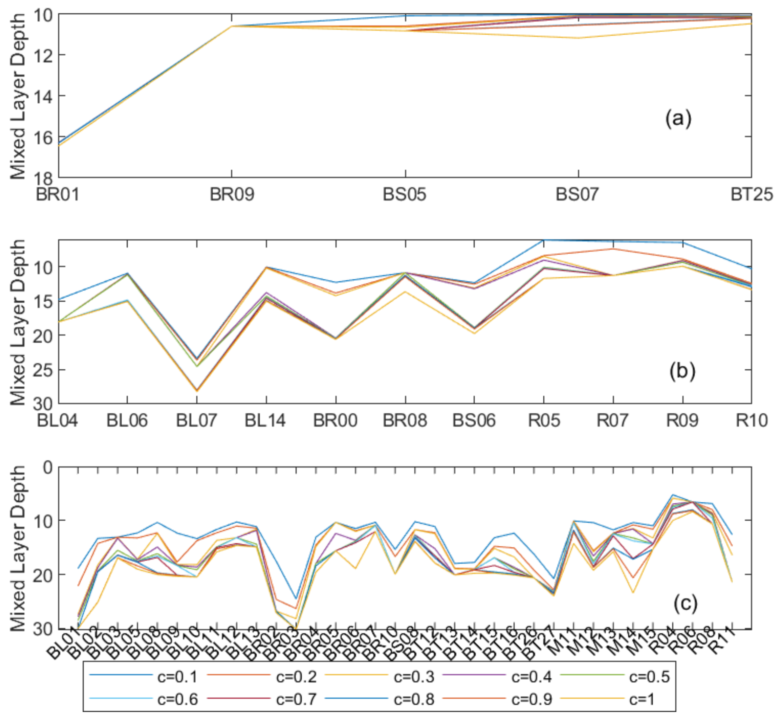

Figure 4. The sensitivity of the MLDt at different stations to criteria is different. (a) Type A: different stations had almost the same MLDt for different criteria; (b) Type B: stations had several MLD around the local extremum calculated by using different criteria; (c) Type C: The MLDt calculated from different criteria changed uniformly with the criteria. The variable c in the legend represented the temperature criteria which ranged from 0.1 to 1 °C.

2.4. Stratification index

The MLD is constrained by the stratification of the ocean. To explore the role of the temperature and the salinity in the stratification, a stratification index was calculated. It

https://doi.org/10.5194/os-2021-7
Preprint. Discussion started: 15 February 2021

is defined as the potential energy of a water column relative to the completely mixed state (Ladd & Stabeno, 2012):

$$V = -\int_{-h}^{0} \left(\rho - \langle\rho\rangle\right) gzdz \tag{1}$$

$$\langle\rho\rangle = \frac{1}{h}\int_{-h}^{0} \rho dz \tag{2}$$

where ρ is the seawater density, and h is the depth of the water column. For a vertically completely mixed water column, V=0. The warmer and fresher the ocean surface is, the greater V is. Wind stress and negative buoyancy flux may strengthen vertical mixing (Prasad, 2004), and make V smaller. Changes in the salinity and temperature both lead to variations of stratification. Their contributions to stratification were explored. For the stratification index due to temperature (salinity), the density profile ρ is calculated using the temperature (salinity) profile and a vertically averaged salinity (temperature).

3. Result analysis

3.1. The salinity and temperature

The spatial variation of MLD is closely related to hydrography and ocean dynamics. The temperature and salinity characteristics between the Bering Sea basin and the continental shelf were significantly different (Figure 5 and Figure 6). The temperature and salinity profiles showed that the seawater in the upper ocean in the Bering Sea Basin was warmer and saltier than that in the Bering Sea Shelf (Figure 5). The sea surface temperature and salinity had a similar pattern (Figure 6). The upper ocean above 30 m in the Bering Sea basin had the characteristics of high temperature and low salinity. The sea surface temperature was about 11.5 ℃ and the sea surface salinity was about 33 in the Bering Sea basin, while they were 10.5 ℃ and 32.2 respectively in the Bering Sea shelf. There was a cold water mass with a depth range of 50-200m and a core temperature slightly lower than 3 ℃ in the middle layer. The temperature of the bottom cold water mass in the southern continental shelf was similar to that of the

https://doi.org/10.5194/os-2021-7
Preprint. Discussion started: 15 February 2021

middle cold water mass in the basin, but the bottom cold water mass was shallower due to terrain constraints on the shelf. The temperature of the bottom cold water mass decreased from 3 ℃ in the south to 1 ℃ in the north.

The hydrographic features between the northeast and northwest of the continental shelf were different. There was a cold water mass with a core temperature of 2 ℃ in the west, and the salinity was higher than 32.5. In the east, the temperature was higher than 9 ℃ and the salinity was significantly lower than that in the west. In the east, the density of high-temperature and low-salinity water was smaller, which had the characteristics of the Alaska Coastal Water. It might be affected by the Yukon River's freshwater. The density of low-temperature and high-salinity water on the west side was larger and had the characteristics of the Anadyr Water.

There were high-temperature and low-salinity water masses with the temperature range of 1~10 ℃ and salinity of 28~30 in the upper layer of the Chukchi Sea shelf and the continental slope (Figure 8). The sea surface temperature gradually decreased from 10 ℃ in the south to 2 ℃ in the north and the sea surface salinity decreased from 30 to 28 from south to north. There was a low-temperature and high-salinity water mass on the bottom. The temperature of the bottom water decreased from 4 to -1.3 ℃ from south to north, while the salinity also decreased from 32 to 30 (Figure 8). There was a middle cold water mass with a core temperature of -1.8 ℃ in the depth range of 40m ~ 150m below the surface warm water in the Chukchi Sea slope.

3.2. Characteristics of MLD in the Bering Sea

The spatial distributions of MLD between the basin located in the southwest of the Bering Sea and the continental shelf located in the northeast had significantly different characteristics.

The BL section was representative due to its wide span of space. The stations BL02 - BL06 were located in the Bering Sea basin, and the MLD at these stations were all greater than 15 m (Figure 7 (a)). The maximum value of the MLD in the Bering Sea basin reached 18.72 m, and it was observed at the BL02 station located in the southern

https://doi.org/10.5194/os-2021-7
Preprint. Discussion started: 15 February 2021

Bering Sea basin. The MLDd and MLDt had little difference at stations BL02 - BL05, but the difference between the MLDd and the MLDt approached 4 m at BL06 station (Figure 7 (d)). In contrast, the MLD observed at stations BL11 - BL14 which were located in the west of the Bering Sea shelf was shallower than 15 m. And the minimum of the MLD at the BL section was 6.23 m, which was observed at BL14 station. The BL14 station was located in the northwestern Bering Sea shelf. It should be noted that the MLDt (14.30 m) is much larger than MLDd (6.25 m) at BL14 station. The maximum of the MLD at the BL section was 30.03 m. It occurred at the BL01 station, which was located in the continental slope on the north of the Aleutian Island. The MLD at BL07 station located in the Bering Sea slope was 25.32 m. Both of the MLD at BL01 and BL07 stations were markedly larger than those MLD in the Bering Sea basin and the Bering Sea shelf.

The stations BR00 - BR03 were on the Bering Sea slope. The maximum MLD reached 30.17 m, and it occurred at BR03 station (Figure 7 (b)). The minimum MLD was 16.32 m at these stations and almost larger than all the MLD in the Bering Sea shelf, including the stations BR04 - BR10. The average MLD at stations BR04 - BR09 was 13.72 m, much smaller than the 23.44 m in the Bering Sea slope. The stations BR10 and BR11 were in the northeast of the Bering Sea shelf, and it can be seen that the isohaline and the isothermal were almost vertical there (Figure 5 (b) and (e)). Corresponding to that, the MLD at BR10 and BR11 stations were dramatically greater than those at other BR stations in the Bering Sea shelf.

The western BS section was under the influence of the water mass named Anadyr Water in the northwestern Bering Sea, and the eastern BS section was under the influence of the Alaska Coastal Water in the northeastern Bering Sea. Thus the BS section represented the MLD under the influence of the advection of these two water masses. As the water column at BS01 - BS03 was well-mixed, the MLD were all larger than 35 m. On the contrary, the MLDt was zero there. The MLD in the northeast was much smaller and had a value of 6 m - 13 m. As the denser Anadyr Water intruded eastward under the Alaska Coastal Water (Figure 5 (c)), the MLD in the transition zone,

https://doi.org/10.5194/os-2021-7
Preprint. Discussion started: 15 February 2021

including stations BS04 and BS05, was smaller (Figure 7 (c)). It should be noted that the MLDt was significantly greater than MLDd in the northeastern Bering Sea shelf.

Overall, the MLD in the Bering Sea basin was greater than those on the continental shelf. The MLD in the continental slope of the Bering Sea was significantly greater than those in the basin and the continental shelf. The MLD was larger than 30 m as the water column was well-mixed in the northwestern Bering Sea shelf, but the MLD decreased toward the east. The MLDd was generally larger than MLDt in the Bering Sea basin, the Bering Sea slope, and the southern Bering Sea shelf. But in the northern Bering Sea shelf, the MLDt was significantly larger than MLDd.

https://doi.org/10.5194/os-2021-7
Preprint. Discussion started: 15 February 2021

Ocean Science
Discussions
Open Access
EGU

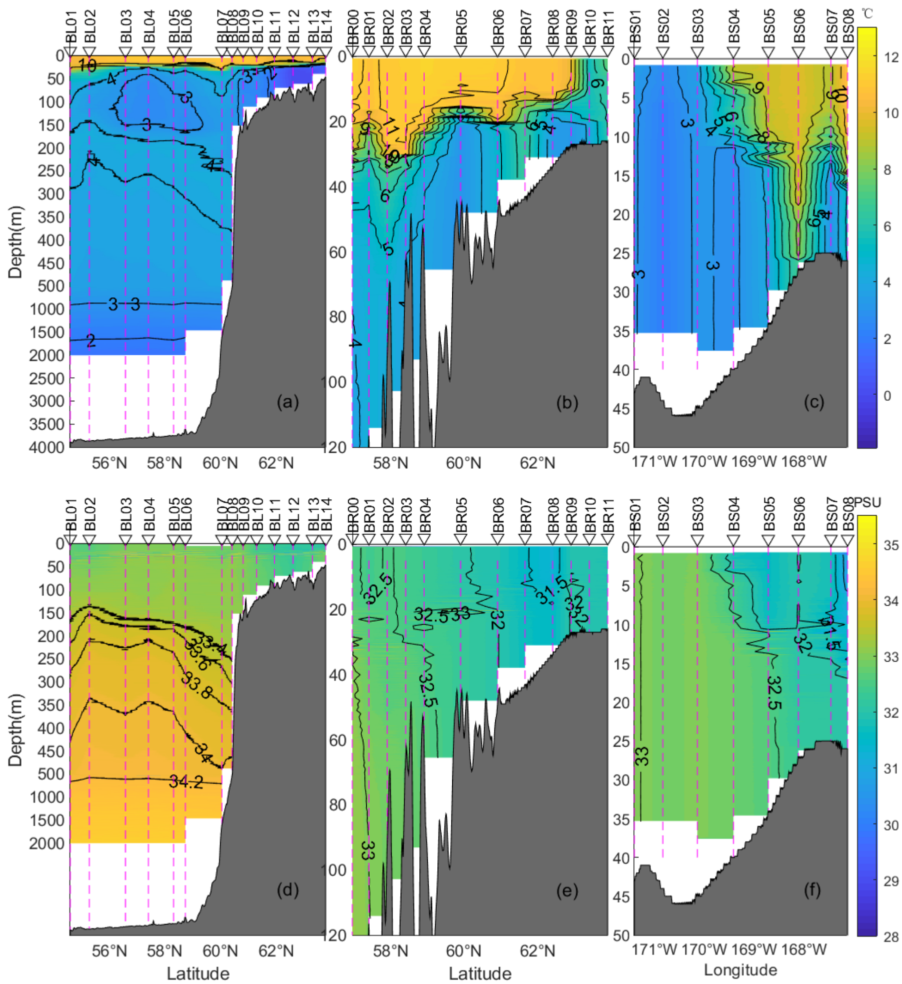

Figure 5 The upper panels and the lower panels represent the temperature and salinity profiles, respectively. The left (a, d), middle (b, e), and right (c, f) column represent the section of BL, BR, and BS, respectively.

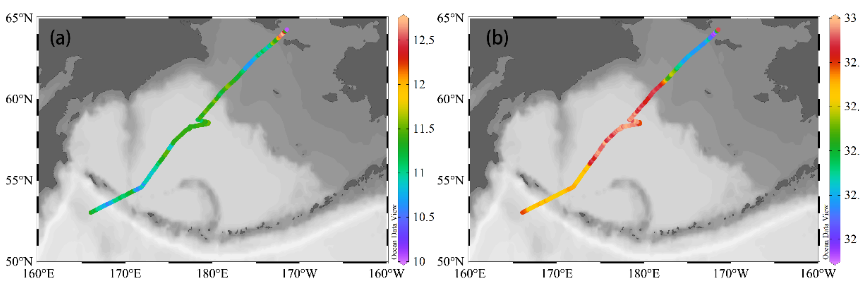

Figure 6. The sea surface temperature (a) and salinity (b) in the Bering Sea.

https://doi.org/10.5194/os-2021-7
Preprint. Discussion started: 15 February 2021

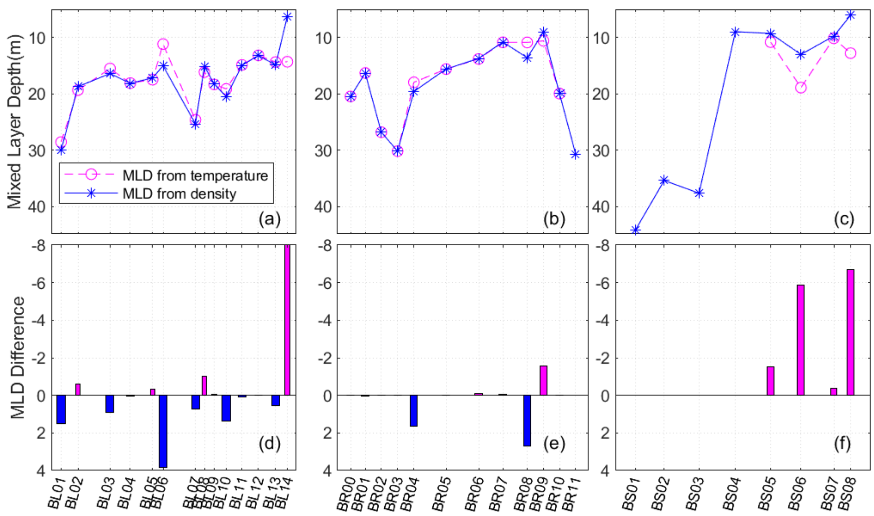

Figure 7. The upper panel represents the MLD from temperature and density. The lower panel represents the difference between MLDd and MLDt. The left (a, d), middle (b, e), and right (c, f) column represent the section of BL, BR, and BS respectively. The magenta dash lines represent the MLD calculated from the temperature, and the blue solid lines represent the MLD calculated from the density. The magenta bar means that the MLDt is larger than the MLDd, and the blue bar means that the MLDd is larger than the MLDt. Notice that the Y-axis is reversed.

3.3. Characteristics of MLD in the Chukchi Sea

The Chukchi Sea is on the north of the Bering Strait. The depth of the continental shelf in the south is about 50 m and it spans several hundreds of kilometers. The MLD at the R section was in the range of 4-12 m. In general, the MLD increased at a rate of 4.5×10^{-6} northward along the R section (Figure 9 (a)).

The northward increase was also observed in the BT section. The maximum MLD was 19.74 m at BT15 station. The MLD at stations BT13-BT16 was all greater than 15 m and was also greater than the MLD in the Chukchi Sea shelf (Figure 9 (c)).

The M section was located to the west of the BT section, and the water depth increased from about 323 m at M11 station to 2123 m at M14 station. The MLD at M section was in the range of 5-10 m, much shallower than that at the BT section (Figure 9 (b)).

The MLD in the Chukchi Sea shelf had an overall trend of deepening from south to north (Figure 9 (a) and (c)). The MLD in the southern Chukchi Sea shelf was smaller than 12 m, and the MLD reached a maximum of 19.74 m in the northern Chukchi Sea shelf. The MLD in the western continental slope was in the range of 5-10 m, similar to that in the southern Chukchi Sea shelf. It seemed that the fluctuation of MLD in the Chukchi Sea slope was not similar to that in the Bering Sea slope.

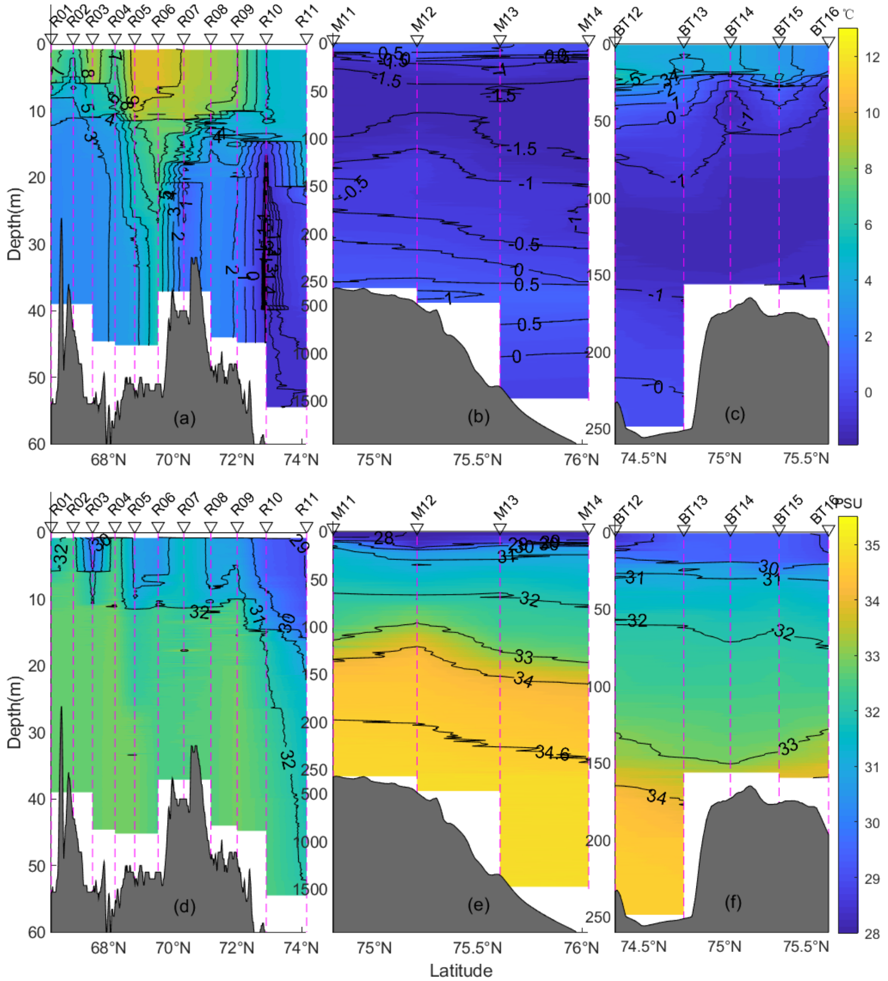

Figure 8. The upper panels and the lower panels show temperature and salinity profiles, respectively. The left (a, d), middle (b, e), and right (c, f) column represent the section of R, M, and BT, respectively.

https://doi.org/10.5194/os-2021-7
Preprint. Discussion started: 15 February 2021

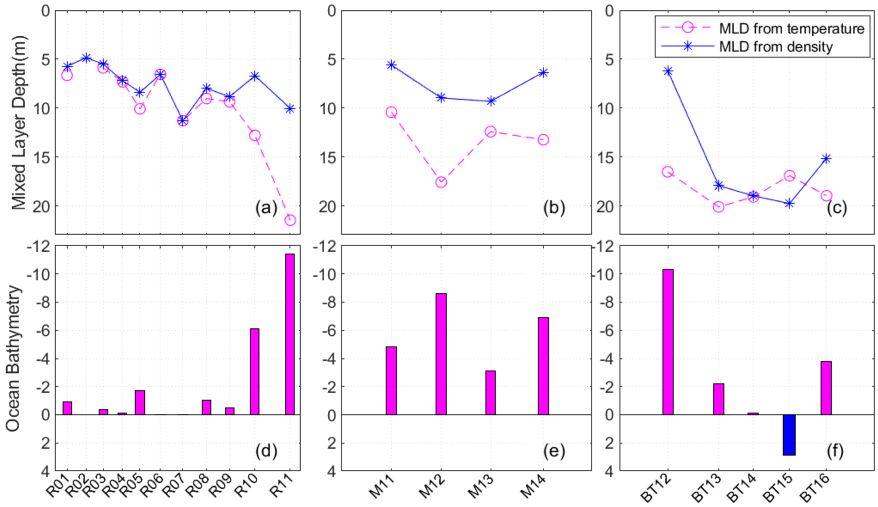

Figure 9. The upper panel represents the MLD from temperature and density. The lower panel represents the difference between MLDd and MLDt. The left (a, d), middle (b, e), and right (c, f) column represent the section of R, M, and BT respectively. The magenta dash lines represent the MLD calculated from the temperature, and the blue solid lines represent the MLD calculated from the density. The magenta bar means that the MLDt was larger than the MLDd, and the blue bar means that the MLDd was larger than the MLDt. Notice that the Y-axis is reversed.

In conclusion, the MLDt was different from MLDd (Figure 7 and Figure 9). The MLDd was generally larger than the MLDt in the southern Bering Sea, while the MLDt was generally larger than the MLDd in the northern Bering Sea shelf and the Chukchi Sea. The average difference between MLDd and MLDt was 0.51 m in the southern Bering Sea, and the average difference is -3.25 m in the northern Bering Sea shelf and the Chukchi Sea. The largest difference between MLDd and MLDt was less than 4 m in the southern Bering Sea, while the largest difference between MLDt and MLDd was greater than 11 m in the Chukchi Sea. The difference between MLDt and MLDd showed a tendency to increase from south to north in the Chukchi Sea.

3.4. The relation of temperature, salinity, and MLD

In this section, the relationships between the spatial variation of MLD and the temperature and salinity were explored.

https://doi.org/10.5194/os-2021-7
Preprint. Discussion started: 15 February 2021

The bottom cold water in the Bering Sea shelf was shallower than the middle cold water mass in the Bering Sea basin. As a result, both the isopycnal and MLD were shallower in the Bering Sea shelf than those in the Bering Sea basin. The MLD in the Bering Sea shelf fluctuated with the topography. Therefore, the shallower MLD in the Bering Sea shelf might be due to the terrain constraints and the bottom friction.

The isothermal and the isohaline showed a trend of deepening in the Bering Sea slope, and the cold water mass in the middle layer also showed a trend of deepening (Figure 5 (a)). As a result, the MLD in the Bering Sea slope was larger than that in the Bering Sea basin (Figure 7(a)).

The density of the Anadyr Water was vertically uniform in the northwestern Bering Sea shelf and was much larger than that of the Alaska Coastal Water in the northeastern Bering Sea shelf. Due to the significant difference in density between the Anadyr Water and the Alaska Coastal Water, advection occurred and the low-density water in the east advected toward the west in the surface water, and high-density water in the west advected toward the east at the bottom. Therefore, the seawater was stratified in the transition zone. As a result, The MLD in the transition zone was shallower than that in the northeastern and northwestern Bering Sea shelf (Figure 7 (c)).

The northward increase of the MLD in the Chukchi Sea was accompanied by the high meridional gradient of the salinity and temperature. That might be the result of the advection of the low-salinity water in the Chukchi Sea. The larger MLD at R05 and R07 stations were related to the high-temperature and low-salinity water mass appearing within the range of 68.5 - 70.5°N on the bottom.

Although the MLD increased in the Chukchi Sea slope as that in the Bering Sea slope, there was a difference between them. It was remarkable that, from the ocean basin towards the continental shelf, the isotherm and isohaline tended to parallel to the continental slope in the Chukchi Sea, while they tended to perpendicular to the continental slope in the Bering Sea. Therefore, it was reasonable to assume that the reason for the deepening of the mixed layer in the Chukchi Sea slope might be different

https://doi.org/10.5194/os-2021-7
Preprint. Discussion started: 15 February 2021

from that in the Bering Sea slope. The changes of MLD in the Chukchi Sea slope might be related to the low-salinity water generated from the melting of sea ice in summer and topographical constraints. But in the Bering Sea slope, the isotherm, isohaline, and MLD were mainly affected by the Bering Slope Current.

The MLDt was generally smaller than MLDd in the southern Bering Sea. This indicated that the temperature constrained the mixed layer in the southern Bering Sea. In other words, the change in density was mainly caused by the change in temperature. The average difference between MLDd and MLDt was -3.25 m in the northern Bering Sea and the Chukchi Sea, the absolute value of which was much greater than the 0.51 m in the southern Bering Sea. It indicated that the MLD was dominated by the salinity in the northern Bering Sea and the Chukchi Sea. Besides, the farther north, the greater the difference between the MLDt and MLDd was in the Chukchi Sea, and the more important role the salinity played in determining the MLD.

4. Discussion on the factors influencing MLD

4.1. Stratification

The contribution of the salinity and the temperature to the MLD was explored by studying the stratification index. The stratification index covered a depth of 60 m, and for the areas shallower than 60 m, it covered the whole water column from the sea bottom to the surface. The temperature interpreted 30%-40% of the stratification in the Bering Sea basin and the southern Bering Sea shelf including BL01-BL13, BR00-BR06, as shown in Figure 10 (a) and (b). In the northeastern Bering Sea shelf and the southern Chukchi Sea shelf, temperature interpreted 10-20% of the stratification (Figure 10 (c) and (d)). In the northern Chukchi Sea shelf, it decreased to 5-10% (Figure 10 (f)). In the Chukchi Sea slope and the northwestern Bering Sea shelf, the contribution of the temperature to stratification was negligible (Figure 10 (c) and (e)). The contribution from salinity to stratification and MLD increased northward in the upper ocean of the Bering Sea and the Chukchi Sea. This is consistent with the previous research (Johnson et al., 2012), which showed that the seasonal variation of

https://doi.org/10.5194/os-2021-7
Preprint. Discussion started: 15 February 2021

Ocean Science
Discussions
Open Access
EGU

the mixed layer in the Arctic was dominated by salinity. Therefore, it is reasonable to assume that the characteristics of the mixed layer are related to the low-salinity water generated from the melting of sea ice in the Chukchi Sea and the northern Bering Sea shelf in the summer of 2019.

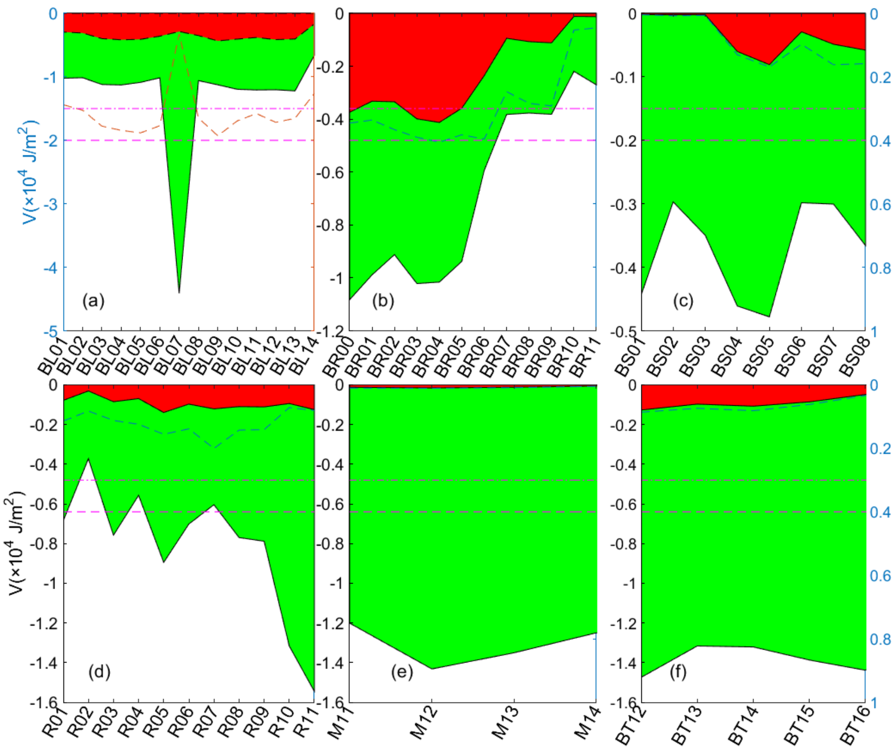

Figure 10. The left axis represented the stratification index. Red was the proportion of stratification due to temperature. Green was the proportion due to salinity. The right axis represented the proportion of the contribution of the temperature. The magenta dash-dotted line and the dashed line represented the proportion of 30% and 40% respectively.

4.2. Circulation and eddy

The deepening of the MLD in the Bering Sea slope might be related to the strengthening of the turbulent mixing caused by the BSC and the strong vorticity along the BSC (Figure 11 and Figure 12 (b)). As shown in Figure 11, the absolute dynamic topography showed a high gradient along the Bering Sea slope. And the current velocity along the Bering Sea slope was about 0.1 m/s, which was significantly larger

https://doi.org/10.5194/os-2021-7
Preprint. Discussion started: 15 February 2021

than that in the Bering Sea basin and the Bering Sea shelf. The large MLD at BL01 in the northern continental slope of the Aleutian Islands was probably related to the eddies along the Aleutian Islands (Figure 12). The MLD at BL01 was 30.04 m, significantly larger than that at BL02, which was 18.72 m (Figure 7 (a)). The current velocity at BL01 was about 0.2 m/s and was larger than that in the basin, which was smaller than 0.1 m/s, according to our ADCP observations.

On the basin scale, the dominant cyclonic circulation might lead to the MLD in the central part of the Bering Sea basin smaller than that in the continental slope in the rim of the basin.

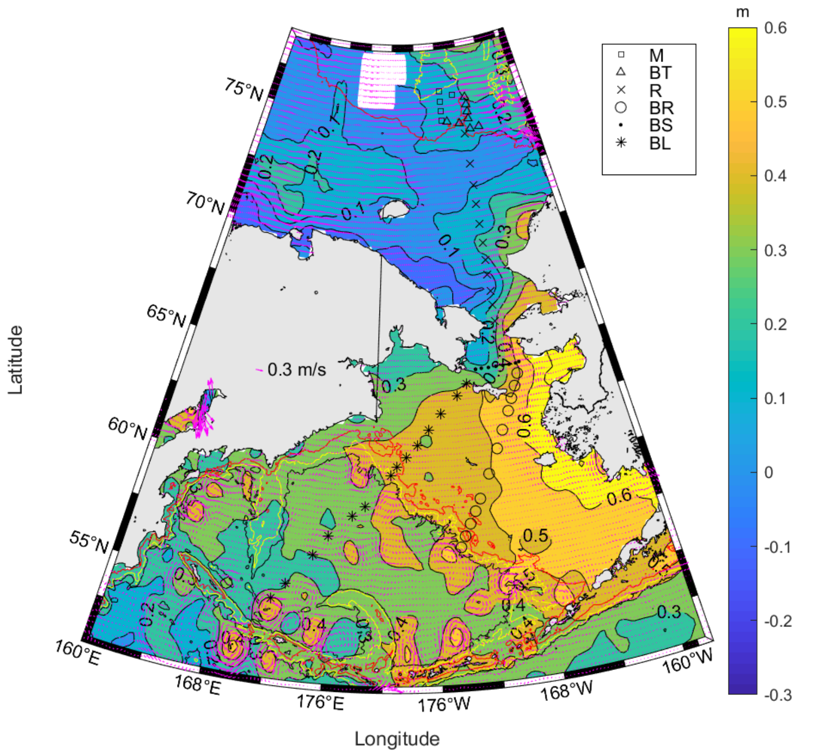

Figure 11. The 16-day averaged absolute dynamic topography and the surface geostrophic flow in the Bering Sea and the Chukchi Sea from satellite altimeter.

https://doi.org/10.5194/os-2021-7
Preprint. Discussion started: 15 February 2021

Ocean Science
Discussions
Open Access

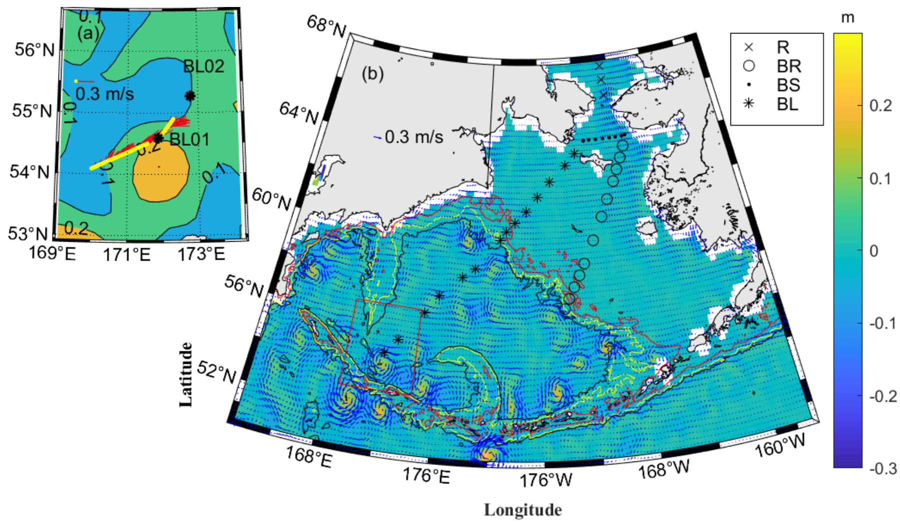

Figure 12. (a) The eddy next to station BL01. The contours denoted the sea surface height from satellite observations. The yellow line denoted the track of the ship. The red vectors denoted the ocean current velocity observed by ADCP. (b) The surface eddy street along the Bering Sea slope from the 16-day averaged SLA. The vectors represented the surface geostrophic flow anomaly. The color denoted the relative vorticity normalized by the local Coriolis coefficient. The red, yellow, and blue solid lines denoted the 200m, 2000m, and 3000m isobaths, respectively. The red rectangle denoted the location of the region in (a).

4.3. Momentum flux and buoyancy flux

In summer, the Aleutian Low moved northward and the south wind prevailed. The wind observed by the shipborne automatic meteorological station was used to assess the CCMP wind product. The correlation coefficients of the zonal wind and meridional wind between them were 0.92 and 0.91 respectively. And the mean difference of the zonal wind and meridional wind between them were 0.51 m/s and 0.29 m/s respectively. That meant the CCMP wind product behaved well in the target region.

The strengthening or weakening of stratification caused by the air-sea kinetic energy exchange on the surface of the ocean changed the MLD. In the west of the Bering Sea basin, in the northeast of the Bering Sea, and the north of the Chukchi Sea (BL, BS, BT, and M stations), the MLD had a positive correlation with the wind speed, and the correlation coefficient was 0.7 (Figure 13). The kinetic energy input into the ocean due

https://doi.org/10.5194/os-2021-7
Preprint. Discussion started: 15 February 2021

Ocean Science
Discussions

to the large wind speed enhanced the sea surface turbulent mixing. As a result, the MLD increased, and BR, BT2, BL01, and BL07 were excluded. It had been known that the MLD at BL01 and BL07 was mainly due to the influence of the continental slope current.

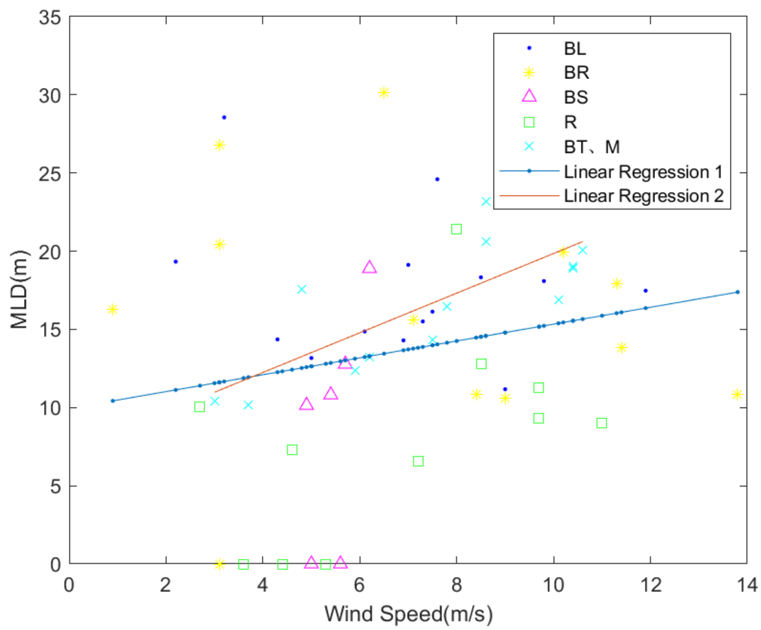

Figure 13. Scatter plot of wind speed and MLD. It contained BL, BS, BT, and M stations. The solid blue line was the regression line.

The relationship between the MLD and the buoyancy flux as well as the momentum flux was explored through Multiple Linear Regression (MLR). When the freshwater and heat content of the upper ocean increased, the stratification was strengthened, and the MLD decreased. When the momentum flux increased, the MLD became larger. The average buoyancy flux caused by sea surface net heat flux and freshwater flux from July 1 to Sept. 8 was shown in Figure 14. The momentum flux from Aug. 15 to Sept. 8 was shown as well. The correlation coefficient between the MLD and momentum flux was 0.67, while the correlation coefficient between the MLD and buoyancy flux was -0.33. Under the combined effect of buoyancy flux and momentum flux, the MLD could reach a regional extremum, such as BL14, BR00, BR11, BT12, BT25, BT26,

https://doi.org/10.5194/os-2021-7
Preprint. Discussion started: 15 February 2021

M11, R01, R05, R08, R11 in Figure 14. The result of multiple linear regression had a correlation coefficient of 0.41 with the measured MLD. As the yellow box in Figure 14 showed, the disappearance of the temperature mixed layer in the northwestern Bering Sea shelf might also be related to momentum flux and buoyancy flux.

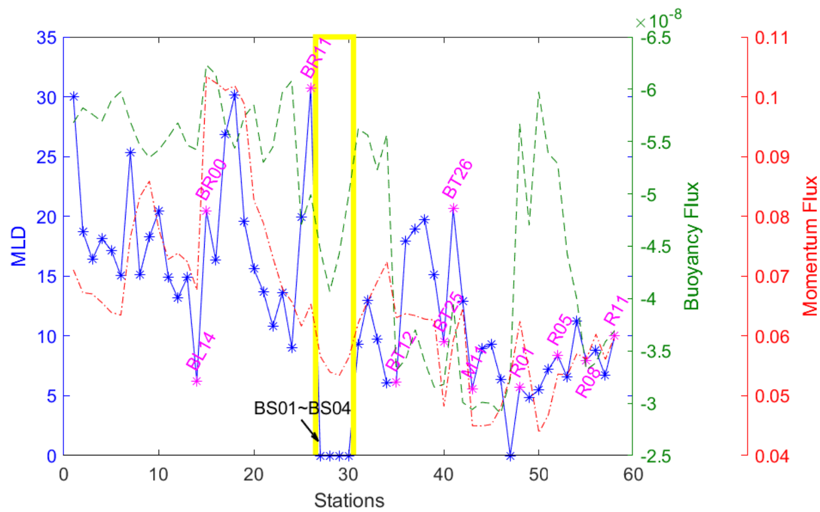

Figure 14. The buoyancy flux, momentum flux, and MLD of all stations. The buoyancy flux is one-month averaged, and the momentum flux is 10-day averaged. The order of stations is the same as Table 3.

4.4. Waves

It seemed that the spatial variation of MLD was not largely affected by the waves during the expedition. It might be because the significant wave height was too small to influence the MLD at that time, and the significant wave height was smaller than 2 m in this region (Figure 15). The consideration of the wave had almost no improvement for the result of the above multiple linear regression. Satellite observations showed a larger significant wave height in the Bering Sea slope and the southeastern Bering Sea. The significant wave height at BR00~BR04 and BL07~BL09 was larger than that in other areas. But the MLD at BR00, BR01, BR04, BL08, BL09 was not large. The correlation coefficient between the significant wave height and MLD was less than 0.05. The addition of the wave made no positive contribution to the multiple linear regression between MLD and momentum flux, buoyancy flux.

https://doi.org/10.5194/os-2021-7
Preprint. Discussion started: 15 February 2021

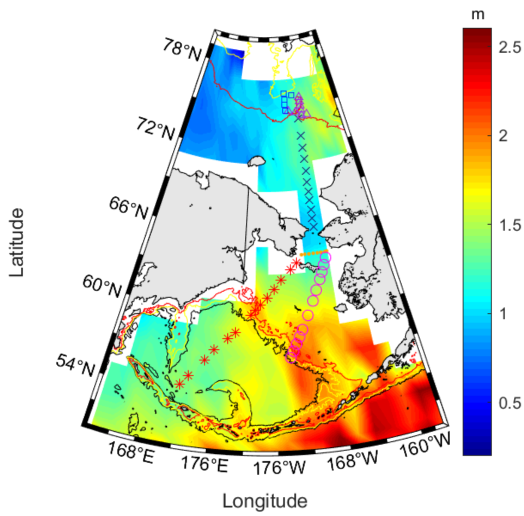

Figure 15. Mean significant wave height during the expedition (from Aug. 24 to Sept. 08).

5. Conclusion

The density threshold of $0.125\ \mathrm{kg}/m^3$ was used to determine the MLD in the Bering Sea and the Chukchi Sea.

The in-situ data showed that the MLD in the Bering Sea basin was deeper than that in the Bering Sea shelf, but both were shallower than that in the Bering Sea slope. In the Chukchi Sea shelf, the MLD deepened from south to north. The mixed layer in the Chukchi Sea slope was similar to that in the southern Chukchi Sea shelf. The deeper mixed layer at the R05 and R07 stations was related to the high-temperature and low-salinity water masses extending from the east.

The factors that dominated the spatial variation of MLD in the Bering Sea and the Chukchi Sea were different. The MLD was constrained by the temperature and the salinity of seawater in the southern Bering Sea, while it was mainly constrained by salinity in the northern Bering Sea and the Chukchi Sea. Therefore, the upper oceanic processes relating to the MLD were different. The larger MLD in the Bering Sea slope was mainly caused by the circulation and eddies, while the MLD in the Chukchi Sea slope was mainly shaped by the spread of the northern low-salinity seawater and the

https://doi.org/10.5194/os-2021-7
Preprint. Discussion started: 15 February 2021

terrain constraints. The MLD in the northern Bering Sea shelf was affected by the interaction of the high-density Anadyr Water and the low-density Alaska coastal water. Overall, the horizontal advection led to the shallower mixed layer in the east and central transition zone. The disappearance of the temperature mixed layer in the northwestern Bering Sea shelf might be related to weak wind, momentum flux, and buoyancy flux. The correlation coefficient between the momentum flux and the MLD was 0.67, larger than that between the buoyancy flux and the MLD, which was -0.33. The correlation coefficient between the wind and MLD reached 0.7, excluding the stations that were obviously affected by eddy and circulation. The wave was not closely related to the spatial variation of the MLD. The combined contributions of both the momentum flux and the buoyancy flux interpreted the local extremum of the MLD.

Data availability

I would like to share my data to scientific community through Harvard Dataverse (https://doi.org/10.7910/DVN/H07MTR). CCMP Version-2.0 vector wind analyses are produced by Remote Sensing Systems. Data are available at www.remss.com. CFSv2 data was retrieved from NCAR Research Data Archive (https://rda.ucar.edu/datasets/ds094.0/). The sea surface height and the significant wave height was obtained from http://marine.copernicus.eu website. The ETOPO1 was obtained from https://www.ngdc.noaa.gov/mgg/global/global.html website.

Author contribution

Xiaohui Jiao performed the in situ observations, analyzed the data and prepared the manuscript. Jicai Zhang gave expert guidance on research orientation. Chunyan Li provided suggestions to improve the analysis and polish the language.

Competing interests

The authors declare that they have no conflict of interest.

https://doi.org/10.5194/os-2021-7
Preprint. Discussion started: 15 February 2021

Ocean Science
Discussions

Acknowledgments

We are extremely grateful to the chief scientist Professor Wei Zexun for his guidance and support. We are very grateful to Liu Na, Chen Hongxia, and He Yan from the First Institute of Oceanography for their help. This work was supported by the National Key Research and Development Plan of China [grant number 2017YFC1404000 and 2017YFA0604100], and the National Natural Science Foundation of China [grant number 41876086 and 41206001].

https://doi.org/10.5194/os-2021-7
Preprint. Discussion started: 15 February 2021

Ocean Science
Discussions

References

Amante, C. and Eakins, B.W.: ETOPO1 1 Arc-Minute Global Relief Model: Procedures, Data Sources and Analysis, NOAA Technical Memorandum NESDIS NGDC-24, National Geophysical Data Center, NOAA, https://doi.org/10.7289/V5C8276M. 2009.

Belcher, S. E., Grant, A. L. M., Hanley, K. E., Fox-Kemper, B., Van Roekel, L., Sullivan, P. P., Large, W. G., Brown, A., Hines, A., Calvert, D., Rutgersson, A., Pettersson, H., Bidlot, J., Janssen, P. A. E. M., & Polton, J. A.: A global perspective on Langmuir turbulence in the ocean surface boundary layer. *Geophysical Research Letters*, *39*, L18605, https://doi.org/10.1029/2012GL052932, 2012.

Bruneau, N., & Toumi, R.: A fully-coupled atmosphere-ocean-wave model of the Caspian Sea, *Ocean Modelling*, *107*, 97-111, https://doi.org/10.1016/j.ocemod.2016.10.006, 2016.

Carton, J. A., Grodsky, S. A., & Liu, H.: Variability of the Oceanic Mixed Layer, 1960–2004, *Journal of Climate*, *21*(5), 1029-1047, https://doi.org/10.1175/2007JCLI1798.1, 2008.

Chen, D., Busalacchi, A. J., & Rothstein, L. M.: The roles of vertical mixing, solar radiation, and wind stress in a model simulation of the sea surface temperature seasonal cycle in the tropical Pacific Ocean, *Journal of Geophysical Research: Oceans*, *99*(C10), 20345-20359, https://doi.org/10.1029/94JC01621, 1994.

Coachman, L. K., & Aagaard, K.: On the water exchange through Bering Strait, *Limnology and Oceanography*, *11*(1), 44-59, https://doi.org/10.4319/lo.1966.11.1.0044, 1966.

Coachman, L. K., and Charnell, R. L.: On Lateral Water Mass Interaction-A Case Study, Bristol Bay, Alaska. *Journal of Physical Oceanography*, 9, 278–297, https://doi.org/10.1175/1520-0485(1979)009<0278:OLWMIC>2.0.CO;2., 1979.

Danielson, S. L., Weingartner, T. J., Hedstrom, K. S., Aagaard, K., Woodgate, R., Curchitser, E., & Stabeno, P. J.: Coupled wind-forced controls of the Bering–Chukchi shelf circulation and the Bering Strait throughflow: Ekman transport, continental shelf waves, and variations of the Pacific–Arctic sea surface height gradient, *Progress in Oceanography*, *125*, 40-61, https://doi.org/10.1016/j.pocean.2014.04.006, 2014.

D'Asaro, E. A.: Turbulence in the Upper-Ocean Mixed Layer, *Annual Review of Marine Science*, *6*(1), 101-115, https://doi.org/10.1146/annurev-marine-010213-135138, 2014.

de Boyer Montégut, C., Madec, G., Fischer, A. S., Lazar, A., & Iudicone, D.: Mixed layer depth over the global ocean: An examination of profile data and a profile-based climatology, *Journal of Geophysical Research: Oceans*, *109*, C12003, https://doi.org/10.1029/2004JC002378, 2004.

Deardorff, J. W., Willis, G. E., & Lilly, D. K.: Laboratory investigation of non-steady penetrative convection, *Journal of Fluid Mechanics*, *35*(1), 7-31, https://doi.org/10.1017/S0022112069000942, 1969.

Dong, C., Gao, X., Zhang, Y., Yang, J., Zhang, H., & Chao, Y.: Multiple-Scale Variations of Sea Ice and Ocean Circulation in the Bering Sea Using Remote Sensing Observations and Numerical Modeling, *Remote Sensing,* 11(12), 1484, https://doi.org/10.3390/rs11121484, 2019.

DuVivier, A. K., Large, W. G., & Small, R. J.: Argo Observations of the Deep Mixing Band in the Southern Ocean: A Salinity Modeling Challenge, *Journal of Geophysical Research: Oceans*, *123*(10), 7599-7617. https://doi.org/10.1029/2018JC014275, 2018.

Fasham, M. J. R., Ducklow, H. W., & McKelvie, S. M.: A nitrogen-based model of plankton dynamics in the oceanic mixed layer, *Journal of Marine Research*, *48*(3), 591-639, https://doi.org/10.1357/002224090784984678, 1990.

Fauchereau, N., Tagliabue, A., Bopp, L., & Monteiro, P. M. S.: The response of phytoplankton biomass to transient mixing events in the Southern Ocean, *Geophysical Research Letters*, *38*(17), https://doi.org/10.1029/2011GL048498, 2011.

Frankignoul, C., & Hasselmann, K.: Stochastic climate models, Part II Application to sea-surface temperature anomalies and thermocline variability, *Tellus*, *29*(4), 289-305. https://doi.org/10.1111/j.2153-3490.1977.tb00740.x, 1977.

Gaube, P., J. McGillicuddy Jr., D., & Moulin, A. J.: Mesoscale Eddies Modulate Mixed Layer Depth Globally, *Geophysical Research Letters*, *46*(3), 1505-1512, https://doi.org/10.1029/2018GL080006, 2019.

Hanawa, K., & Toba, Y.: Terms governing temperature and thickness of the oceanic mixed layer and their estimates for sea areas south of Japan, *Deep Sea Research Part B. Oceanographic Literature Review*, *30*(12), 904, https://doi.org/10.1016/0198-0254(83)96368-9, 1981.

Hanawa, K., & D. Talley, L.: Chapter 5.4 Mode waters, in *International Geophysics*, edited by Siedler, G., Church, J. & Gould, J., pp. 373-386, Academic Press, https://doi.org/10.1016/S0074-6142(01)80129-7, 2001.

Holte, J., Talley, L. D., Gilson, J., & Roemmich, D.: An Argo mixed layer climatology and database. *Geophysical Research Letters*, *44*(11), 5618-5626, https://doi.org/10.1002/2017GL073426, 2017.

Hosoda, S., Ohira, T., Sato, K., & Suga, T.: Improved description of global mixed-layer depth using Argo profiling floats, *Journal of Oceanography*, *66*(6), 773-787, https://doi.org/10.1007/s10872-010-0063-3, 2010.

Hu, A., Meehl, G. A., Otto-Bliesner, B. L., Waelbroeck, C., Han, W., Loutre, M., Lambeck, K., Mitrovica, J. X., & Rosenbloom, N.: Influence of Bering Strait flow and North Atlantic circulation on glacial sea-level changes, *Nature Geoscience*, *3*(2), 118-121, https://doi.org/10.1038/ngeo729, 2010.

Hu, H., & Wang, J.: Modeling effects of tidal and wave mixing on circulation and thermohaline structures in the Bering Sea: Process studies. *Journal of Geophysical Research: Oceans*, *115*(C1). https://doi.org/10.1029/2008JC005175, 2010.

Jiao, X. H.: Replication Data for Observational Study on the Variability of Mixed Layer Depth in the Bering Sea and the Chukchi Sea in the Summer of 2019, V1, Harvard Dataverse, https://doi.org/10.7910/DVN/H07MTR, 2020.

Johnson, G. C., Schmidtko, S., & Lyman, J. M.: Relative contributions of temperature and salinity to seasonal mixed layer density changes and horizontal density gradients, *Journal of Geophysical Research: Oceans*, *117*(C4). https://doi.org/10.1029/2011JC007651, 2012.

Kachel, N. B., Hunt, G. L. Jr., Salo, S. A., Schumacher, J. D., Stabeno, P. J., & Whitledge, T. E.: Characteristics and variability of the inner front of the southeastern Bering Sea, *Deep Sea Research Part II*, **49**(26), 5889–5909, https://doi.org/10.1016/S0967-0645(02)00324-7, 2002.

Kara, A. B., Rochford, P. A., & Hurlburt, H. E.: Mixed layer depth variability and barrier layer formation over the North Pacific Ocean, *Journal of Geophysical Research: Oceans*, *105*(C7), 16783-16801, https://doi.org/10.1029/2000JC900071, 2000.

Kato, H., & Phillips, O. M.: On the penetration of a turbulent layer into stratified fluid, *Journal of Fluid Mechanics*, *37*(4), 643-655, https://doi.org/10.1017/S0022112069000784, 1969.

Kawaguchi, Y., Nishioka, J., Nishino, S., Fujio, S., Lee, K., Fujiwara, A.: Cold water upwelling near the Anadyr Strait: Observations and simulations, *Journal of Geophysical Research: Oceans*, 125, e2020JC016238, https://doi.org/10.1029/2020JC016238, 2020.

Kinder, T. H., & Coachman, L. K.: The front overlaying the continental slope in the eastern Bering Sea, *Journal of Geophysical Research*, 83, 4551–4559, https://doi.org/10.1029/JC083iC09p04551, 1978.

Kraus, E. B., & Turner, J. S.: A one-dimensional model of the seasonal thermocline II, The general theory and its consequences, *Tellus*, *19*(1), 98-106, https://doi.org/10.3402/tellusa.v19i1.9753, 1967.

Ladd, C., & Stabeno, P. J.: Stratification on the Eastern Bering Sea shelf revisited, *Deep Sea Research Part II: Topical Studies in Oceanography*, 65-70, 72-83, https://doi.org/10.1016/j.dsr2.2012.02.009, 2012.

Large, W. G., McWilliams, J. C., & Doney, S. C.: Oceanic vertical mixing: A review and a model with a nonlocal boundary layer parameterization, *Reviews of Geophysics*, *32*, 363, https://doi.org/10.1029/94RG01872, 1994.

Li, S., Song, J., & Fan, W.: Effect of Langmuir circulation on upper ocean mixing in the South China Sea, *Acta Oceanologica Sinica*, *32*(3), 28-33, https://doi.org/10.1007/s13131-013-0285-5, 2013.

Lorbacher, K., Dommenget, D., Niiler, P. P., & Köhl, A.: Ocean mixed layer depth: A subsurface proxy of ocean-atmosphere variability, *Journal of Geophysical Research: Oceans*, *111*(C7), https://doi.org/10.1029/2003JC002157, 2006.

Lukas, R., & Lindstrom, E, The mixed layer of the western equatorial Pacific Ocean, *Journal of Geophysical Research: Oceans*, *96*(S01), 3343-3357, https://doi.org/10.1029/90JC01951, 1991.

Markus, T., Stroeve, J. C., & Miller, J.: Recent changes in Arctic sea ice melt onset, freezeup, and melt season length, *Journal of Geophysical Research: Oceans*, *114*(C12), https://doi.org/10.1029/2009JC005436, 2009.

McWilliams, J. C., Sullivan, P. P., & Moeng, C.: Langmuir turbulence in the ocean, *Journal of Fluid Mechanics*, *334*, 1-30, https://doi.org/10.1017/S0022112096004375, 1997.

McWilliams, J. C., Huckle, E., & Shchepetkin, A. F.: Buoyancy Effects in a Stratified Ekman Layer, *Journal of Physical Oceanography*, *39*(10), 2581-2599, https://doi.org/10.1175/2009JPO4130.1, 2009.

Mizobata, K., Wang, J., & Saitoh, S.: Eddy-induced cross-slope exchange maintaining summer high productivity of the Bering Sea shelf break, *Journal of Geophysical Research: Oceans*, *111*(C10), https://doi.org/10.1029/2005JC003335, 2006.

Monterey, G. A. S. L.: *Seasonal Variability of Mixed Layer Depths for the World Ocean*, 96 pp., U.S. Government Prinitng Office, Washington, D.C., 1997.

Ohlmann, J. C., Siegel, D. A., & Gautier, C.: Ocean Mixed Layer Radiant Heating and Solar Penetration: A Global Analysis, *Journal of Climate*, *9*(10), 2265-2280, https://doi.org/10.1175/1520-0442(1996)009<2265:OMLRHA>2.0.CO;2, 1996.

Okkonen, S. R.: Altimeter observations of the Bering Slope Current eddy field, *Journal of Geophysical Research: Oceans*, *106*(C2), 2465-2476, https://doi.org/10.1029/2000JC000285, 2001.

Overland, J. E., Stabeno, P. J., & Salo, S.: Direct evidence for northward flow on the northwestern Bering Sea shelf, *Journal of Geophysical Research: Oceans*, *101*(C4), 8971-8976, https://doi.org/10.1029/96JC00205, 1996.

Panteleev, G., Yaremchuk, M., Luchin, V., Nechaev, D., & Kukuchi, T.: Variability of the Bering Sea circulation in the period 1992–2010, *Journal of Oceanography*, *68*(4), 485-496, https://doi.org/10.1007/s10872-012-0113-0, 2012.

Peralta-Ferriz, C., & Woodgate, R. A.: Seasonal and interannual variability of pan-Arctic surface mixed layer properties from 1979 to 2012 from hydrographic data, and the dominance of stratification for multiyear mixed layer depth shoaling. *Progress in Oceanography*, *134*, 19-53. https://doi.org/10.1016/j.pocean.2014.12.005, 2015.

Polyakov, I. V., Pnyushkov, A. V., Rember, R., Padman, L., Carmack, E. C., & Jackson, J. M.: Winter Convection Transports Atlantic Water Heat to the Surface Layer in the Eastern Arctic Ocean, *Journal of Physical Oceanography*, *43*(10), 2142-2155, https://doi.org/10.1175/JPO-D-12-0169.1, 2013.

Prasad, T. G.: A comparison of mixed-layer dynamics between the Arabian Sea and Bay of Bengal: One-dimensional model results, *Journal of Geophysical Research: Oceans*, 109(C03035C3), https://doi.org/10.1029/2003JC002000, 2004.

Price, J. F., Weller, R. A., & Pinkel, R.: Diurnal cycling: Observations and models of the upper ocean response to diurnal heating, cooling, and wind mixing, *Journal of Geophysical Research: Oceans*, *91*(C7), 8411-8427, https://doi.org/10.1029/JC091iC07p08411, 1986.

Roach, A. T., Aagaard, K., Pease, C. H., Salo, S. A., Weingartner, T., Pavlov, V., & Kulakov, M.: Direct measurements of transport and water properties through the Bering Strait, *Journal of Geophysical Research: Oceans*, *100*(C9), 18443-18457, https://doi.org/10.1029/95JC01673, 1995.

Rodgers, K. B., Aumont, O., Fletcher, S. E. M., Plancherel, Y., Bopp, L., de Boyer Mont E Gut, C., Iudicone, D., Keeling, R. F., Madec, G., & Wanninkhof, R.:

https://doi.org/10.5194/os-2021-7
Preprint. Discussion started: 15 February 2021

Strong sensitivity of Southern Ocean carbon uptake and nutrient cycling to wind stirring. *Biogeosciences*, *11*(15), 4077-4098, https://doi.org/10.5194/bg-11-4077-2014, 2014.

Rodionov, S. N., Bond, N. A., & Overland, J. E.: The Aleutian Low, storm tracks, and winter climate variability in the Bering Sea, *Deep Sea Research Part II: Topical Studies in Oceanography*, *54*(23), 2560-2577, https://doi.org/10.1016/j.dsr2.2007.08.002, 2007.

Saha, S., Moorthi, S., Wu, X., Wang, J., Nadiga, S., Tripp, P., Behringer, D., Hou, Y., Chuang, H., Iredell, M., Ek, M., Meng, J., Yang, R., Mendez, M. P., van den Dool, H., Zhang, Q., Wang, W., Chen, M., and Becker, E.: updated daily, NCEP Climate Forecast System Version 2 (CFSv2) 6-hourly Products. Research Data Archive at the National Center for Atmospheric Research, Computational and Information Systems Laboratory, https://doi.org/10.5065/D61C1TXF, 2011.

Schmidtko, S., Johnson, G. C., & Lyman, J. M.: MIMOC: A global monthly isopycnal upper-ocean climatology with mixed layers, *Journal of Geophysical Research: Oceans*, *118*(4), 1658-1672, https://doi.org/10.1002/jgrc.20122, 2013.

Schumacher, J. D., Kinder, T. H., Pashinski, D. J., & Charnell, R. L.: A structural front over the continental shelf of the eastern Bering Sea, *Journal of Physical Oceanography*, **9**(1), 79–87,https://doi.org/10.1175/1520-0485(1979)009<0079:ASFOTC>2.0.CO;2, 1979.

Schumacher, J., & Stabeno, P. J.: The continental shelf of the Bering Sea, In A. R. Robinson & K. H. Brink (Eds.), *The Sea: The Global Coastal Ocean Regional Studies and Synthesis* (Vol. 11, pp. 869–909), New York: John Wiley, 1998.

Serreze, M. C., Barrett, A. P., Slater, A. G., Woodgate, R. A., Aagaard, K., Lammers, R. B., Steele, M., Moritz, R., Meredith, M., & Lee, C. M.: The large-scale freshwater cycle of the Arctic, *Journal of Geophysical Research: Oceans*, *111*(C11), https://doi.org/10.1029/2005JC003424, 2006.

Serreze, M. C., Crawford, A. D., Stroeve, J. C., Barrett, A. P., & Woodgate, R. A.: Variability, trends, and predictability of seasonal sea ice retreat and advance in the Chukchi Sea, *Journal of Geophysical Research: Oceans*, *121*(10), 7308-7325, https://doi.org/10.1002/2016JC011977, 2016.

Shaffer, G., & Bendtsen, J.: Role of the Bering Strait in controlling North Atlantic ocean circulation and climate, *Nature*, *367*(6461), 354-357, https://doi.org/10.1038/367354a0, 1994.

Sirevaag, A., de la Rosa, S., Fer, I., Nicolaus, M., Tjernström, M., and McPhee, M. G.: Mixing, heat fluxes and heat content evolution of the Arctic Ocean mixed layer, *Ocean Science*, 7, 335–349, https://doi.org/10.5194/os-7-335-2011, 2011.

Smyth, W. D., Hebert, D., & Moum, J. N.: Local ocean response to a multiphase westerly wind burst: 2. Thermal and freshwater responses, *Journal of Geophysical Research: Oceans*, *101*(C10), 22513-22533, https://doi.org/10.1029/96JC02006, 1996.

Stabeno, P. J., & Reed, R. K.: Circulation in the Bering Sea Basin Observed by Satellite-Tracked Drifters: 1986–1993, *Journal of Physical Oceanography*, *24*(4), 848-854, https://doi.org/10.1175/1520-0485(1994)024<0848:CITBSB>2.0.CO;2,

https://doi.org/10.5194/os-2021-7
Preprint. Discussion started: 15 February 2021

1994.

Stevenson, J. W., & Niiler, P. P.: Upper Ocean Heat Budget During the Hawaii-to-Tahiti Shuttle Experiment, *Journal of Physical Oceanography*, *13*(10), 1894-1907, https://doi.org/10.1175/1520-0485(1983)013<1894:UOHBDT>2.0.CO;2, 1983.

Stommel, H.: Determination of water mass properties of water pumped down from the Ekman layer to the geostrophic flow below, *Proceedings of the National Academy of Sciences of the United States of America*, *76*(7), 3051-3055, https://doi.org/10.1073/pnas.76.7.3051, 1979.

Sverdrup, H. U.: On Conditions for the Vernal Blooming of Phytoplankton, *Ices Journal of Marine Science*, *18*(3), 287-295, https://doi.org/10.1093/icesjms/18.3.287, 1953.

Thomson, R. E., & Fine, I. V.: Estimating Mixed Layer Depth from Oceanic Profile Data, *Journal of Atmospheric and Oceanic Technology*, *20*(2), 319-329, https://doi.org/10.1175/1520-0426(2003)020<0319:EMLDFO>2.0.CO;2, 2003.

Tully, J. P.: Oceanographic Regions and Assessment of Temperature Structure in the Seasonal Zone of the North Pacific Ocean, *Journal of the Fisheries Research Board of Canada*, *21*(5), 941-970, https://doi.org/10.1139/f64-089, 1964.

Visbeck, M.: Deep Velocity Profiling Using Lowered Acoustic Doppler Current Profilers: Bottom Track and Inverse Solutions*, *Journal of Atmospheric and Oceanic Technology*, 19(5), 794-807, https://doi.org/10.1175/1520-0426(2002)019<0794:DVPULA>2.0.CO;2, 2002.

Wadley, M. R., & Bigg, G. R.: Impact of flow through the Canadian Archipelago and Bering Strait on the North Atlantic and Arctic circulation: An ocean modelling study, *Quarterly Journal of the Royal Meteorological Society*, *128*(585), 2187-2203, https://doi.org/10.1256/qj.00.35, 2002.

Wentz, F.J., J. Scott, R. Hoffman, M. Leidner, R. Atlas, J. Ardizzone.: Remote Sensing Systems Cross-Calibrated Multi-Platform (CCMP) 6-hourly ocean vector wind analysis product on 0.25 deg grid, Version 2.0. Remote Sensing Systems, Santa Rosa, CA. Available online at www.remss.com/measurements/ccmp, 2015

Wijesekera, H. W., & Gregg, M. C.: Surface layer response to weak winds, westerly bursts, and rain squalls in the western Pacific warm pool, *Journal of Geophysical Research: Oceans*, *101*(C1), 977-997, https://doi.org/10.1029/95JC02553, 1996.

Woodgate, R. A., Aagaard, K., & Weingartner, T. J.: A year in the physical oceanography of the Chukchi Sea: Moored measurements from autumn 1990–1991, *Deep Sea Research Part II: Topical Studies in Oceanography*, *52*(24), 3116-3149, https://doi.org/10.1016/j.dsr2.2005.10.016, 2005.

Woodgate, R. A., Weingartner, T., & Lindsay, R.: The 2007 Bering Strait oceanic heat flux and anomalous Arctic sea-ice retreat, *Geophysical Research Letters*, *37*(1), https://doi.org/10.1029/2009GL041621, 2010.

Woodgate, R. A., Weingartner, T. J., & Lindsay, R.: Observed increases in Bering Strait oceanic fluxes from the Pacific to the Arctic from 2001 to 2011 and their impacts on the Arctic Ocean water column, *Geophysical Research Letters*, *39*(24), https://doi.org/10.1029/2012GL054092, 2012.

Woodgate, R. A.: Increases in the Pacific inflow to the Arctic from 1990 to 2015, and insights into seasonal trends and driving mechanisms from year-round Bering Strait mooring data, *Progress in Oceanography*, *160*, 124-154, https://doi.org/10.1016/j.pocean.2017.12.007, 2018.

Wu, L., Rutgersson, A., & Sahlée, E.: Upper-ocean mixing due to surface gravity waves, *Journal of Geophysical Research: Oceans*, *120*(12), 8210-8228, https://doi.org/10.1002/2015JC011329, 2015.

Zhang, J., Woodgate, R., & Moritz, R.: Sea Ice Response to Atmospheric and Oceanic Forcing in the Bering Sea, *Journal of Physical Oceanography*, *40*(8), 1729-1747, https://doi.org/10.1175/2010JPO4323.1, 2010.